

The sub-fossils of leaf fragments in sediments as an indicator of mangrove development in the Yingluo Bay, Guangxi, Southwest China over the last 130 years

Wanzhu Wang¹, Xianwei Meng^{1,2*}, Xiangqin Wang¹, Zhen Li³

¹Laboratory of Marine Sedimentology and Environmental Geology, First Institute of Oceanography, Ministry of Natural Resources, Qingdao 266061, China

²Laboratory for Marine Geology and Environment, Pilot National Laboratory for Marine Science and Technology (Qingdao), Qingdao 266237, China

³School of Earth and Ocean Sciences, University of Victoria, British Columbia V8W, Canada

Received 1 February 2018; accepted 26 March 2018

© Chinese Society for Oceanography and Springer-Verlag GmbH Germany, part of Springer Nature 2019

Abstract

Located in the intertidal zone of the tropical and subtropical coasts, mangrove forests are an important ecosystem in the global carbon cycle and serve as a protector of local seashores. Under the double impacts of climate change, especially sea-level rise, and human activity, mangrove forests around the world have faced degradation, against which the reconstruction of the historical development of mangrove forests using an effective indicator has been regarded as a necessary strategy for designing a predictable model. As the primary product of mangrove forest, it is reasonable that the content of leaf fragments of mangrove (CLFM) buried in sediments in the form of sub-fossils potentially has the same indicative function for the development of mangrove forests as that of widely-used mangrove pollen. In this study, the leaf fragments of mangrove in two sediment cores (YLW02 and YLW03) drilled in the Yingluo Bay in Guangxi, Southwest China were picked out and weighted for calculation of CLFM, which was used as an indicator of mangrove development after examination of parallelism and a statistical correlation of the CLFM with the concentration of mangrove pollen. The results clearly show that the vertical distribution of the CLFM for the core taken from the landward margin of mangrove forests (YLW03) only parallels that of the local mangrove species (*Rhizophora stylosa*) with a significantly positive correlation ($R=0.56$, $P=0.05$), while the vertical distribution of the CLFM for the core taken from the interface between seaward margin of mangrove forest and the trunk of tidal creeks of the bay (YLW02) parallels the summed concentration of mangrove pollen (SCMP) with a more positive correlation than that of YLW03 ($R=0.85$, $P=0.01$), indicating that the trunk outlet of tidal creeks must have been the site where mangrove production gathered from the overall forest rather than from local production. The variations in the CLFM of both cores indicate that overall the mangrove forests in the Yingluo Bay have increasingly flourished over the last 130 years except for the interval of 1940–1950 AD in response to an increase in air temperature and decrease in rainfall, which would have resulted in an increase in seawater salinity; while the coupled extreme increases in air temperature and in rainfall in summer, which would have resulted in extreme decreases in seawater salinity, would be responsible for the relative degradation of mangrove forests in the interval of 1940–1950 AD.

Key words: leaf fragment, mangrove development, Yingluo Bay, last 130 years, air temperature and rainfall

Citation: Wang Wanzhu, Meng Xianwei, Wang Xiangqin, Li Zhen. 2019. The sub-fossils of leaf fragments in sediments as an indicator of mangrove development in the Yingluo Bay, Guangxi, Southwest China over the last 130 years. Acta Oceanologica Sinica, 38(8): 27–34, doi: 10.1007/s13131-018-1221-5

1 Introduction

In the face of global climate change, which is receiving considerable attention from governments over the last several decades, an increasing number of scientists have focused on the effects of climate change on mangrove ecosystems. Mangrove forests' characteristic location at the interface between marine and terrestrial ecosystems along tropical and subtropical coastal zones makes them vulnerable to human activity and climate change, in particular to fluctuations in sea level (Ellison and Stoddart, 1991; Ellison, 1993; Parkinson et al., 1994; Yulianto et al., 2004; Gilman et al., 2007). The responses of mangrove ecosystems to future climate change can be understood by reconstructing the dynamics of past mangrove development at different

timescales. The annual development of mangrove forests over recent decades can be directly determined from observational records in the form of satellite imagery; the long-term development of mangrove forests such as over the last 150 years, however, can only be reconstructed from proxy records in mangrove sediments (Ellison, 2008). To date, the concentration of mangrove pollen (CMP) has been proven to be the most straightforward and effective proxy (Li et al., 2008) and is widely used to trace the historical development of mangrove forests during the Holocene (Versteegh et al., 2004; Wooller et al., 2007; Monacci et al., 2009; Ellison, 2008; Li et al., 2012). However, determination of the CMP requires substantial technical expertise and expenditure during the processing and identification of samples (Versteegh et al., 2004; Wooller et al., 2007; Monacci et al., 2009; Ellison, 2008; Li et al., 2012).

Foundation item: The National Natural Science Foundation of China under contract Nos 41376075 and 41576061.

*Corresponding author, E-mail: mxw@fio.org.cn

gh et al., 2004; Wooller et al., 2007; Li et al., 2008). Therefore, its use is sometimes limited to high-resolution studies of the development of mangrove forests, in particular when the pollen concentration is very low (Li et al., 2008). Even though the geochemical proxies for organic matter (OM) in bulk sediments, such as stable organic carbon isotope ($\delta^{13}\text{C}_{\text{org}}$), the ratio of total organic carbon to total nitrogen (C:N ratio), nitrogen isotope ($\delta^{15}\text{N}$) (Lorente et al., 2014; França et al., 2014; Cohen et al., 2016), have been used to complement the CMP in the reconstruction of mangrove development, there remain issues and uncertainties due to organic matter degradation during early sedimentary diagenesis. Therefore, for the study of mangrove development, it is necessary to find an indicator requiring low-technical expertise and low costs.

As the primary product of mangrove forests, leaves can directly reflect the growth status of mangrove forests just as pollen concentrations do. In addition, the high content of tannic acid in mangrove leaves (which accounts for 42% of their dry weight) could have a function that resists the decomposition of organic matter in leaves by microorganisms (González-Farías and Mee, 1988), and hence, mangrove leaves could be preserved during the deposition process in the form of sub-fossils. Therefore, the content of leaf fragments of mangrove (CLFM) in sediments could be theoretically used to trace the history of mangrove evolution. Wooller et al. (2007) first utilized the total area of leaf fragments as the substitutive indicator to trace mangrove forest development. In this way, only the larger leaf fragments (more than 1 mm in diameter) were visually selected and used to estimate the area of visualized leaf fragments for individual sedimentary layers rather than the total leaf fragments. In fact, there are more small invisible leaf fragments in sediments because of the tidal scour action. Therefore, this method is less scientific for tracing mangrove development.

In this study, we chose the CLFM in dry weight in sediments instead of leaf-fragment area as an indicator to trace mangrove development over the last 150 years in the Yingluo Bay, Guangxi, Southwest China on the basis of ^{210}Pb age frames of two sediment cores and concentrations of mangrove pollen, which have

previously been determined by Xia et al. (2015).

2 Materials and methods

2.1 Study sites and sampling

The Yingluo Bay ($21^{\circ}28'\text{N}$, $109^{\circ}43'\text{E}$), a core part of the Shankou Mangrove National Nature Reserve, is located in the coastal zone of the northern Beibu Gulf, in Southwest China (Fig. 1), adjacent to the Leizhou Peninsula. The landform of the bay consists of mangrove flats, bare flats, and tidal creeks, with sediments characterized by silty and sandy-silty clay (Fig. 1).

The regional climate in the Yingluo Bay is characterized as a tropical monsoonal climate with a pronounced maritime influence. The mean annual temperature is 22.4°C , with a maximum of 37.4°C and a minimum of -0.8°C . The average annual rainfall is 1 815 mm, 80%–85% of which occurs during the summer rainy season (April–September). The annual mean evaporation is 1 800 mm with an average relative humidity of 81.8%. The tide is diurnally irregular, with mean flood and ebb tidal ranges of 3.17 m and 4.19 m, respectively. The duration of the flood tide is longer than that of the ebb tide, and the velocity of the flood tide is consequently lower (Meng et al., 2017). The salinity of the tidal water is only affected by monsoonal rainfall and is relatively stable, ranging from 20 to 23 (Meng et al., 2017).

The regional inland vegetation of the study area is typical of tropical forests and includes evergreen monsoon forests and semi-evergreen monsoon forests. However, many of these natural forests have been cleared for human settlement and agricultural cultivation, or have been left to secondary vegetation, including tropical shrubs and grasses. Over 90% of the 25.51-km coastline along the Yingluo Bay is covered by mangrove vegetation (Li et al., 2008). The mangrove distribution is characterized by the zonal transition of the mangrove community from dike (*Excoecaria agallocha*) to upper beach (*Bruguiera gymnorrhiza* and *Rhizophora stylosa*), to middle beach (*Aegiceras corniculatum* and *Kandelia candel*), and to lower beach (*Avicennia marina*). Of all these five species, *K. candel* is predominant and is widely distributes in the bay.

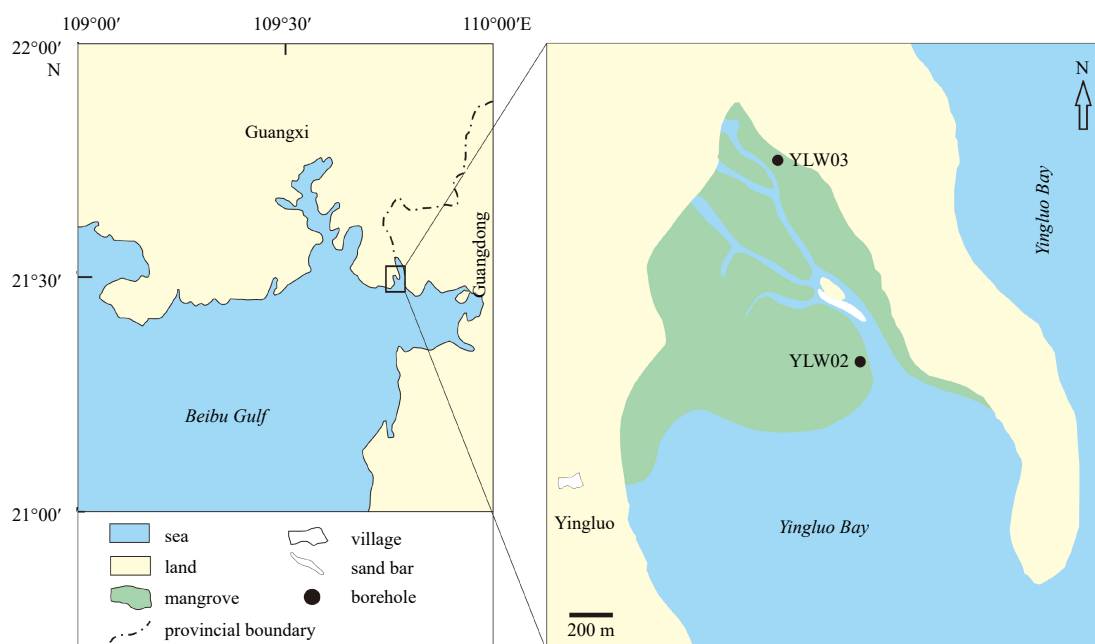


Fig. 1. Sketched map showing the geographic position of the Yingluo Bay, mangrove distribution, and sampling sites.

In this study, two short sediment cores (YLW02 and YLW03) were collected according to the zonal transitions of the mangrove community from the coast to the sea. Core YLW03, with a length of 50 cm, was collected near the landward margin of the mangrove forest in an area, covered by *R. stylosa*; Core YLW02, with a length of 60 cm, was collected at the interface between the seaward margin of the mangrove forest and the trunk of a tidal creek system, at the middle beach (Fig. 1).

According to the profiles of excess ^{210}Pb concentrations ($^{210}\text{Pb}_{\text{ex}}$) (Xia et al., 2015) and the effective age interval of the ^{210}Pb aging method (less than 150 years), the depths prepared for sub-sampling were determined as 45 cm spanning a time interval of 1868 to 2010 AD for Core YLW02, and 36 cm spanning a time interval of 1878 to 2010 AD for Core YLW03. Two cores were cut into subsamples at intervals of 2 cm, each of which were used for analysis of grain size and for picking out leaf fragments of mangrove.

2.2 Analytical methods

Since the data for concentrations of mangrove pollen and ^{210}Pb for each core are available from the literature (Xia et al., 2015), we only describe the analytical methods used to determine grain size and the content of leaf fragment of mangrove.

2.2.1 Grain size analysis

For grain size analysis, aliquots of the subsamples were treated with 10% HCl and 15% H_2O_2 to remove carbonates and organic matter. They were then analyzed using a Malvern 2000 laser-diffraction analyzer in the Key Laboratory of Marine Sedimentology & Environmental Geology, Ministry of Natural Resources. The grain size parameters for each subsample, such as the mean grain size (Mz) and median diameter (Md), were automatically calculated.

2.2.2 Picking out leaf fragments of mangrove

The leaf fragments were picked out under a microscope in the following steps: the subsamples were dried at a temperature of 50°C and weighed using an analytical balance, and then washed with deionized water through a sieve with mesh of $63\ \mu\text{m}$. The remaining detritus in the sieve was freeze-dried; then, the silicate

grain and mangrove roots were identified under a microscope and picked out by hand. As a result, only leaf fragments were left for weighing with an analytical balance. The percentage of leaf fragments in the bulk subsample (W , %) was determined using the following formula:

$$W = 100\% \times m/M, \quad (1)$$

where m and M represent the weight (g) of leaf fragments and bulk subsamples, respectively.

3 Results

3.1 Variations in lithology and grain size

According to the fine division of grain-size grades, the variations in lithology and Md for Cores YLW02 and YLW03 can be divided into two stages: from 1868 to 1910 AD (Stage I), and to 2010 AD (Stage II) for YLW02 (Figs 2a and b), and from 1878 to 1930 AD (Stage I), and to 2010 AD (Stage II) for YLW03 (Figs 2d and e). For Stage I of Core YLW02, the sediments were characterized by clayey silt, and were evenly composed of finer fractions, with averaged Md values of $7.22\ \Phi$, while for Stage II of this core, the sediments abruptly shifted to be sandy silt, with a fluctuant increase in Md (Fig. 2b). For Stage I of Core YLW03, the sediments were characterized by sandy silt, with a slightly increase in Md (Fig. 2e), and then abruptly shifted to become silty sand in Stage II, with a fluctuant decrease in Md (Fig. 2e) in contrast to Stage II of YLW02.

3.2 Variations in the CLFM

The CLFM in Stage I, which had sediments that were composed of finer grain-size fractions, was much lower both for YLW02 and YLW03 and varied evenly or only slightly (Figs 2c and f). However, the CLFM increased in Stage II following the coarsening of grain size for YLW02, and in contrast, it increased following the fining of grain size for YLW03. The effect of grain size on the CLFM was clearly exhibited by their statistical correlations. For YLW02, the CLFM exhibited a negatively significant correlation with Md ($R=0.62$, $P=0.01$, $n=22$) except for one abnormal value at depth of 33 cm (Fig. 3a), indicating that the CLFM

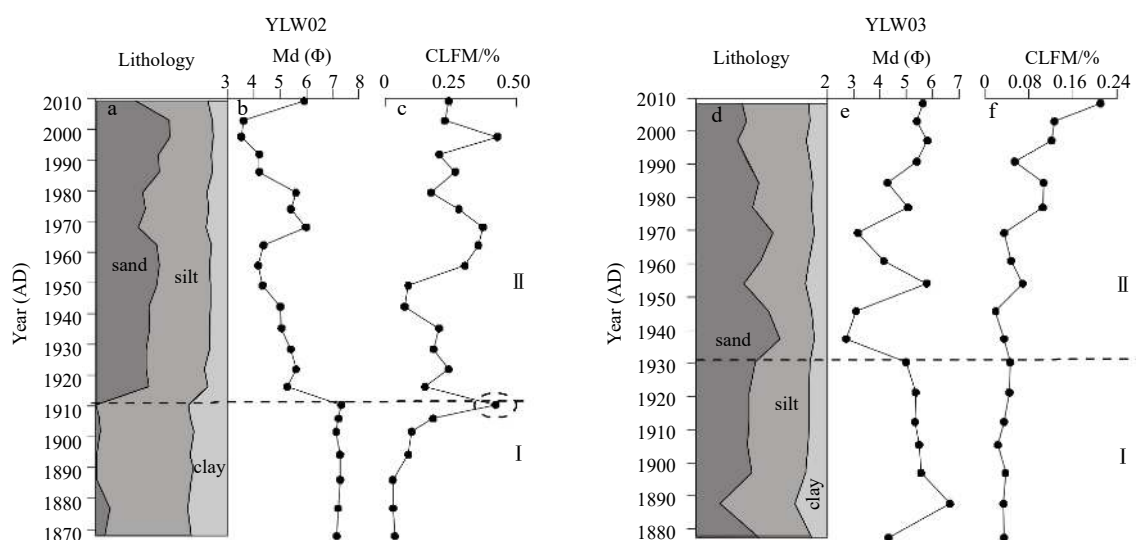


Fig. 2. Variations in lithology (a and d), median grain size (Md) (b and e), and content of leaf fragments of mangrove (CLFM) (c and f) for YLW02 and YLW03, respectively.

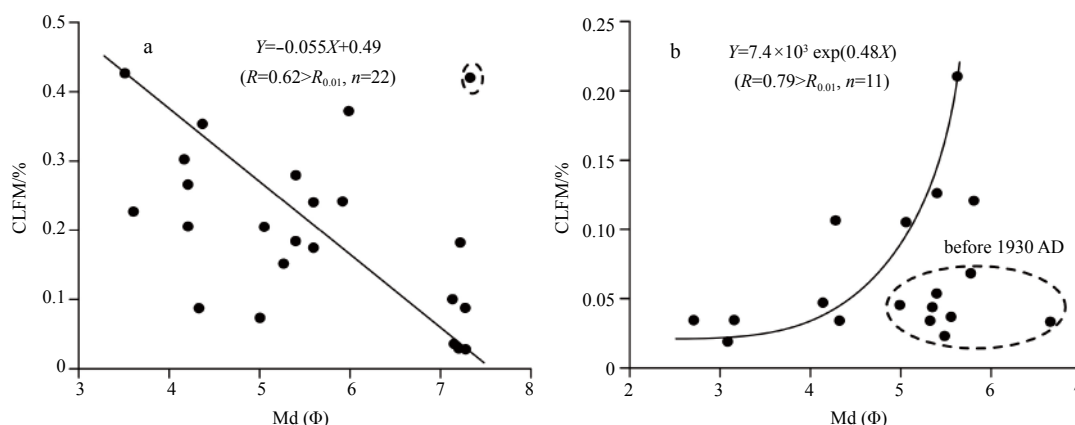


Fig. 3. Plots of CLFM vs. Md for YLW02 (a) and YLW03 (b), showing a significant correlation between the two variables for the entire section (since 1870 AD) of YLW02, and for the upper section (after 1930 AD) of YLW03.

increases with the coarsening of grain size at the site of the interface between the seaward margin of mangrove forest and the trunk of tidal creeks; for YLW03, this correlation only existed for Stage 2 and shifted to become significantly positive (Fig. 3b) ($R=0.79$, $P=0.01$, $n=11$), indicating that the CLFM increases with the fining of grain size after 1930 AD for the site near the landward margin of the mangrove forest.

The more interesting observation is that the CLFM in sediments of YLW02 is much higher than that of YLW03, especially for Stage 2, in which the average values of the CLFM is 0.24% for YLW02 and 0.08% for YLW03.

4 Discussion

In reality, CLFM buried in sediments only represent the remaining fraction of the total leaves that have fallen from plants. The accumulation of this remaining fraction is an outcome of numerous processes, including leaf supply from trees which depends on the stand structure (density and canopy), settlement in tidal water, re-suspension, migration upwards and downwards separately by flood and ebb tides during deposition. All of these processes are site-specific and vary with time in response to climate, especially to relative sea-level (RSL) changes. Therefore, prior to discussing the usefulness of the CLFM as an indicator of mangrove development, we first analyze the influences of hydrodynamic changes on the variations in the CLFM of the two sediments cores.

4.1 The influences of hydrodynamic changes on the variations in the CLFM

Assuming that the amount of leaves falling from the mangrove trees is constant, the duration of inundation by sea water and the tidal or wave current energy associated with the inundation would play important roles in site-specific variation in the CLFM. Longer period of inundation favors additional capture of leaf fragments from mangrove trees. We tentatively interpret the influences of these hydrodynamic conditions on site-specific variations in the CLFM under RSL change by comparing the variations in the CLFM with those in the coefficients of variations (CV) in grain size, which is generally defined as the ratio of the sorting coefficient (δ) to Mz (Meng et al., 2017).

Even though a given site in mangrove forests would theoretically receive falling leaves *in situ* when the site is both exposed and covered by seawater during flood tides, the leaves directly settled on the substrate of the site would be predominately com-

posed of leaves that fall when the site is exposed because leaves falling on the seawater would be apt to be carried away from the site by the ebb tides. The substrate would be eroded, and hence, the settled leaves on the substrate of the site would be broken up, partially re-suspended and carried away from the site by to-and-fro tides. In addition, the site also partially receives the re-suspended and broken-up leaf fragments from adjacent sites in the same way. Waves also play an additional role in the breaking up, re-suspending, and transporting of leaf fragments in the process of the accumulation of the fragments in sediments. That is why the sub-fossil leaves in the sediments of YLW02 and YLW03 are characterized by fragments rather than intact leaves. The quantity and degree of fragmentation depend on the site-specific hydrodynamic conditions.

Core YLW03 was taken from a landward margin where the energies both of flood tides and waves are the relatively weak due to the energy attenuation from seaward to landward margins produced by mangrove trees, while the energy of the ebb tides is strong and the duration of inundation by seawater is the short. However, the Mz (Φ) and δ (Φ) of sediment grain size and their ratio (CV) indicate that the hydrodynamic energy at the site was consistently strong over the last 130 years (Fig. 4) but abruptly becomes weaker after 1945 AD (Fig. 5a), implying that the strong ebb tides and short inundation by sea water would be the predominant factors. These geomorphic and associated hydrodynamic conditions would be responsible for less deposition of leaf fragment at the site of YLW03. The relatively weak energies of both flood tides and waves would make the site receive more falling leaves from the local mangrove species than those re-suspended counterparts from lower-beach sites, while the relatively short inundation by sea water would result in less deposition of leaf fragments of mangrove, which would be re-suspended and then carried away by the strong ebb tide. As a result, the CLFM remaining in sediments of YLW03 was much lower than that of YLW02.

Core YLW02 is located at the interface between seaward margin of mangrove forest and the trunk of tidal creeks. Similar to a river's water system, the trunk is an exchange pathway for material and energy between intertidal mangrove ecosystems and the adjacent sea. Therefore, the site, on the one hand, would receive some re-suspended leaf fragments from the entire bay that were transported in advance into the trunk directly or through creeks during ebb tides, so that the CLFM in sediments of this site was much higher than that of YLW03. On the other hand, the site is

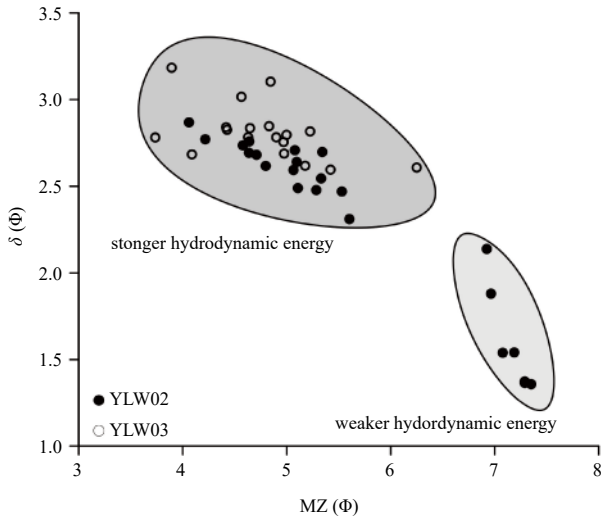


Fig. 4. Plot of sorting coefficient of grain size (δ) vs. mean grain size (Mz) for Cores YLW02 and YLW03, showing two areas of hydrodynamic energy: stronger and weaker areas.

directly influenced by flood tides in response to fluctuant rise of RSL (Smoak et al., 2013), which would make the hydrodynamic energy characterized by CV increase in a wave-like pattern in accordance with RSL (Figs 5b and c) and shift from weaker to stronger status at 1910 AD (Figs 2 and 4). In response to this wave-like increase in the hydrodynamic energy resulting from the fluctuant rise of RSL, the CLFM increased in a wave-like pat-

tern after 1950 AD (Figs 5b and c).

4.2 Mangrove development in the Yingluo Bay over the last 130 years

4.2.1 Validation of the CLFM as an indicator of mangrove development

Prior to the employment of the CLFM as an indicator of mangrove development in the Yingluo Bay, the reliability of this employment was confirmed by a comparison of the parallelism in variations between the CLFM and concentration of mangrove pollen (CMP) in combination with statistical correlation analysis. For this purpose, Stage II, which was determined separately for the two cores according to their variations in grain size (Fig. 2), was further divided into two sub-stages of 1910 to 1950 AD (IIa) and to 2010 AD (IIb) for YLW02 and 1930 to 1990 AD (IIa) and to 2010 AD (IIb) for YLW03 (Fig. 6), such that the change in the average CLFM value of the three intervals can be compared with the change in the CMP for the two cores.

For YLW02, the average CLFM increased from Stage I to IIa, and to II b, in accordance with the values of the CMPs of *A. corniculatum*, *K. candel*, and *B. gymnorrhiza* (Table 1), which account for more than 82% of the summed concentration of mangrove pollen (SCMP). Therefore, the increase in CLFM also parallel to the increase in SCMP (Fig. 6), with a significantly positive correlation ($R=0.85$, $P=0.01$, $n=23$) (Fig. 7a). This result indicates that the measure of CLFM in the sediment core collected at the interface between seaward margin of the mangrove forest and the trunk of the tidal creeks reflects the mangrove development of the entire bay rather than that of the local species or com-

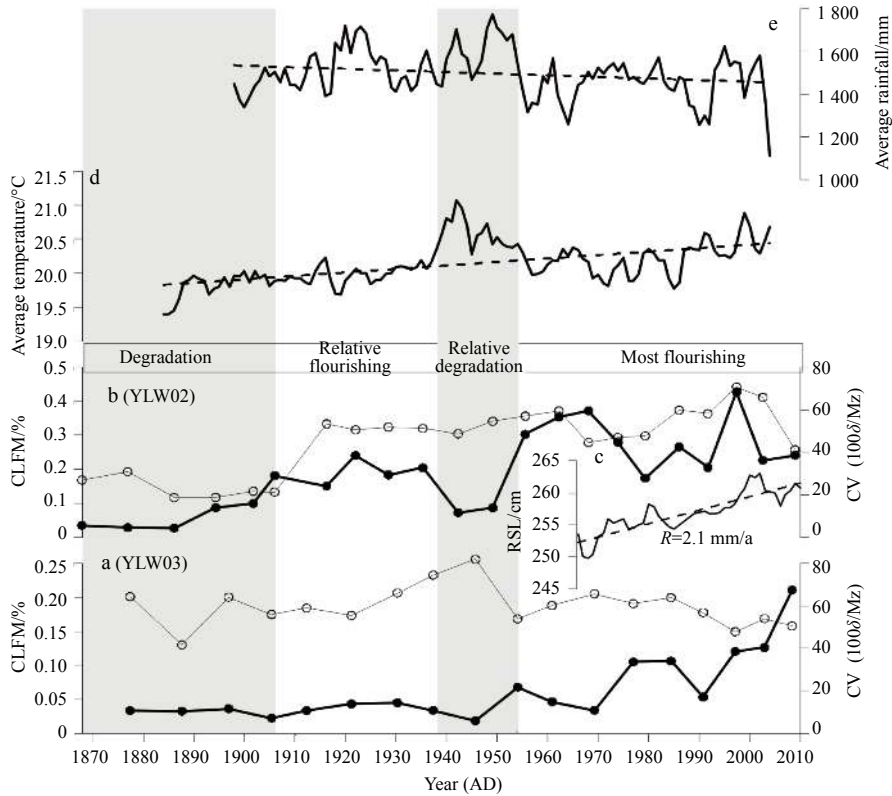


Fig. 5. Mangrove development indicated by CLFM (black dots), with hydrodynamic variation (circles), which is indicated by the ratios of δ to Mz (CV) in the sediments of Cores YLW03 (a) and YLW02 (b), and its response to the rise of relative sea level (RSL) and changes (c) in air temperatures (d) and rainfall (e).

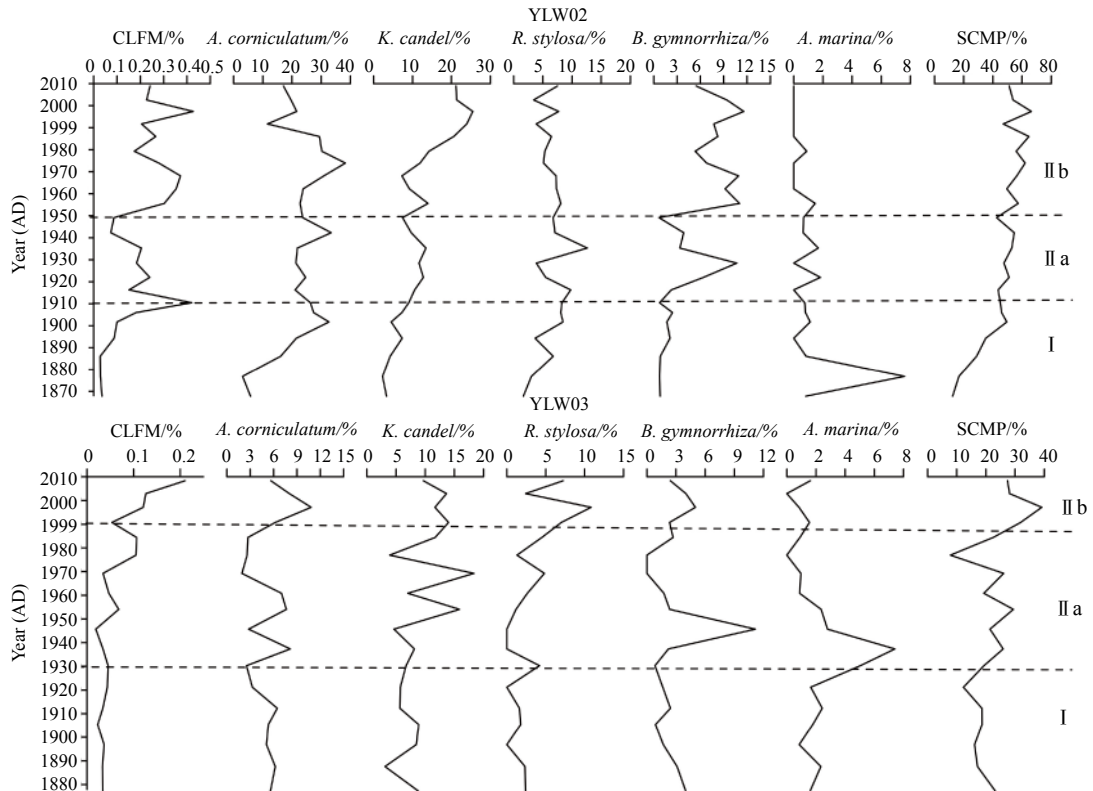


Fig. 6. Comparison of the variation in CLFM with that of CMP and of summed concentration of mangrove pollen (SCMP) both for Cores YLW02 and YLW03. Data of mangrove pollen were cited from Xia et al. (2015).

Table 1. Comparison of CLFM (%) with CMPs (%) and SCMP(%) in three stages for two cores

Core	Stages (AD)	CLFM	<i>A. marina</i>	<i>A. corniculatum</i>	<i>K. candel</i>	<i>R. stylosa</i>	<i>B. gymnorrhiza</i>	SCMP
YLW02	IIb (1950–2010)	0.28	0.24	24.54	16.91	6.21	8.57	56.46
	IIa (1910–1950)	0.16	0.80	24.33	10.91	7.60	4.54	48.75
	I (1968–1910)	0.13	1.71	18.97	5.42	5.70	1.34	33.38
YLW03	IIb (1990–2010)	0.15	0.82	8.17	11.67	6.83	2.81	31.57
	IIa (1930–1990)	0.06	2.11	4.88	10.46	2.68	2.82	23.05
	I (1978–1930)	0.04	2.24	4.93	6.77	1.76	2.09	17.91

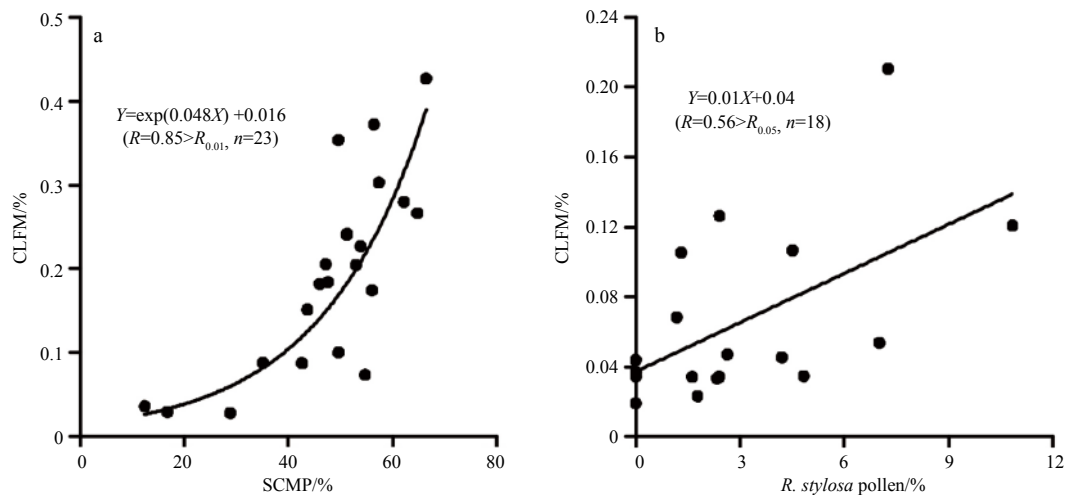


Fig. 7. Plots of CLFM vs. SCMP for YLW02, showing a more significant correlation (a), and CLFM vs. CMP of *R. stylosa* for YLW03, showing a less significant correlation (b).

munity.

For YLW03, even though the average CLFM increased from Stage I to IIa, and to IIb, in accordance with the CMPs of *K. candel* and *R. stylosa* and SCMP (Table 1), the statistical correlation analysis demonstrated that the significantly positive correlation of CLFM to CMP of individual mangrove species and SCMP only exists for *R. stylosa* ($R=0.56$, $P=0.05$, $n=18$) (Fig. 7b), indicating that the CLFM more derived from local *R. stylosa* than those from other species, such as *K. candel*, and hence it only serves as an indicator of local *R. stylosa* development.

4.2.2 Mangrove development

As described above, the cored sediment from the site at the interface between seaward margin of the mangrove forest and the trunk of tidal creeks (YLW02) is useful for describing entire mangrove development in the Yingluo Bay, whereas the cored sediment from the site at the landward margin of the mangrove forest (YLW03) is useful for describing local mangrove development in the Yingluo Bay. However, the CLFM of YLW02 exhibits similar variation to that of YLW03 (Figs 5a and b), indicating that both local and entire mangrove forests have experienced similar development since 1870 AD. This development can be divided into four stages: degradation from 1870 to 1905 AD, relative flourishing from 1905 to 1940 AD, relative degradation from 1940 to 1950 AD, and mostly flourishing since 1950 AD (Fig. 5).

4.3 Influence of climatic changes on mangrove development

The factors influencing mangrove development on a short-term scale, such as over the last 150 years, are usually divided into two categories. One is the so-called natural agents: climate and its associated regional environmental changes; the other is human activity. In the Yingluo Bay, there is no riverine runoff and little human activity along its coasts, the influences of human activity on mangrove development in the bay, therefore, can be considered negligible. Mangrove development since 1870 AD can be attributed to natural agents, including the rise of RSL, changes in air temperature and rainfall, which influences mangrove development through effects on seawater salinity.

4.3.1 Influence of RSL rise on mangrove forests

In general, the rise of RSL can result in a landward extension of mangrove forests and the succession of floral compositions. However, this outcome is primarily controlled by the balance between RSL rise and the mangrove substrate, which primarily depends on the regional sedimentation rate (SR) on short-term scales (Ellison, 2000; 2008). The variation in annual tidal height over the past 50 years at the Beihai Observation Station demonstrates that the RSL rises at a rate of 2.1 mm/a (Fig. 5c), which is approximately equal to the average SR in the Yingluo Bay (2.4 cm/a, Xia et al., 2015). This clearly implies that the increase in the substrate height of the mangrove habitat in the Yingluo Bay has approximately kept pace with the rise of the RSL, so that the mangrove forests have not been influenced by the rise of the RSL over the last 130 years. A study of the landscape evolution of the Guangxi coastal mangroves based on Landsat images over the last 40 years showed no migration of the mangrove forest in the Yingluo Bay (Jia et al., 2015), further supporting that the rise of RSL has not resulted in landward migration of the mangrove forest.

4.3.2 Influences of air temperature and rainfall on the growth of mangrove plants

Under the condition that the accumulation rate of mangrove

substrate keeps pace with the rate of RSL rise, rainfall and air temperature are the primary climate components influencing the growth of mangrove plants (Ellison, 2000; Gilman et al., 2008).

Air temperature influences the growth of mangrove plants through modulation of their photosynthesis. The most appropriate range of air temperature for the growth of mangrove plants is between 28°C and 32°C; both extremely low and high air temperature, which are less than 16°C and higher than 38°C, respectively, are not appropriate for the growth of mangrove plants (Ellison, 2000), and consequently, a longer duration of these extreme climates would result in mangrove degradation.

For a bay where no river enters, such as the Yingluo Bay, rainfall influences the growth of mangrove plants primarily through two ways. One is that it directly influences the growth rates of mangrove plants through modulation of air moisture and thus photosynthesis; the other is that it indirectly influences the growth of mangrove plants through modulation of seawater salinity. In comparison with inland C3 plants, all mangrove species are more competitive in the intertidal zone due to their stronger capability for removing salt rather than their preference to salty environment (Gilman et al., 2008); while the environment with extremely low salinity is also not benefit for competition of mangrove plants with other C3 rivals. Therefore, the highest rainfall and its associated extremely low seawater salinity would be not appropriate for the growth of mangrove plants, especially for the species *A. corniculatum* and *A. marina*.

As a whole, the CLFM of the cored sediments of both YLW03 and YLW02 in the Yingluo Bay have exhibited an increasing trend since 1870 AD except for the interval of 1940–1950 AD (Figs 5a and b), in correspondence with an increase in the average air temperature and a decrease in rainfall, indicating that the mangrove forest in the bay has increasingly flourished since 1870 AD, in response to the increases in average air temperature and seawater salinity. However, the CLFMs of the two cores relatively decreased in the interval of 1940–1950 AD in correspondence with highest air temperature and rainfall (Figs 5a and b), indicating that the relative degradation of the mangrove forest in the bay resulted from the coupled influence of extremely high air temperatures and rainfall in summer in this period.

5 Conclusions

The reconstruction of the historical development using some effective indicator has been regarded as a necessary strategy for designing a predictable model. As the primary product of mangrove forests, the CLFM buried in sediments in the form of sub-fossils has proven to be an effective indicator of mangrove development in the Yingluo Bay over the last 130 years by examination of the parallelism and a statistical correlation of the CLFM with the concentration of mangrove pollen. These results clearly demonstrated that an increase in average air temperature and a decrease in rainfall would be responsible for the increasing flourishing both local and entire mangrove forests since 1870 AD, rather than the rise of the RSL. The coupled extreme increases in the air temperature and rainfall in summer, which would have resulted in an extreme decrease in seawater salinity, would be responsible for the relative degradation of the mangrove forest in the interval of 1940–1950 AD.

References

- Cohen M C L, Lara R J, Cuevas E, et al. 2016. Effects of sea-level rise and climatic changes on mangroves from southwestern littoral of Puerto Rico during the middle and late Holocene. *CATENA*, 143: 187–200, doi: 10.1016/j.catena.2016.03.041

- Ellison J C. 1993. Mangrove retreat with rising sea-level, Bermuda. *Estuarine, Coastal and Shelf Science*, 37(1): 75–87, doi: [10.1006/ecss.1993.1042](https://doi.org/10.1006/ecss.1993.1042)
- Ellison J C. 2000. How South Pacific mangrove may respond to predicted climate change and sea-level rise. In: Gillespie A, Burns W C G, eds. *Climate Changes in South Pacific: Impacts and responses in Australia, New Zealand, and Small Island States*. Dordrecht, Netherlands: Kluwer Academic Publishers, 289–301
- Ellison J C. 2008. Long-term retrospection on mangrove development using sediment cores and pollen analysis: a review. *Aquatic Botany*, 89(2): 93–104, doi: [10.1016/j.aquabot.2008.02.007](https://doi.org/10.1016/j.aquabot.2008.02.007)
- Ellison J C, Stoddart D R. 1991. Mangrove ecosystem collapse during predicted sea-level rise: Holocene analogues and implications. *Journal of Coastal Research*, 7(1): 151–165
- França F C, Francisquini M I, Cohen M C L, et al. 2014. Inter-proxy evidence for the development of the Amazonian mangroves during the Holocene. *Vegetation History and Archaeobotany*, 23(5): 527–524, doi: [10.1007/s00334-013-0420-4](https://doi.org/10.1007/s00334-013-0420-4)
- Gilman E, Ellison J, Coleman R. 2007. Assessment of mangrove response to projected relative sea-level rise and recent historical reconstruction of shoreline position. *Environmental Monitoring and Assessment*, 124(1–3): 105–130
- Gilman E L, Ellison J, Duke N C, et al. 2008. Threats to mangroves from climate change and adaptation options: a review. *Aquatic Botany*, 89(2): 237–250, doi: [10.1016/j.aquabot.2007.12.009](https://doi.org/10.1016/j.aquabot.2007.12.009)
- González-Farias F, Mee L D. 1988. Effect of mangrove humic-like substances on biodegradation rate of detritus. *Journal of Experimental Marine Biology and Ecology*, 119(1): 1–13, doi: [10.1016/0022-0981\(88\)90148-7](https://doi.org/10.1016/0022-0981(88)90148-7)
- Jia Mingming, Wang Zongming, Zhang Yuanzhi, et al. 2015. Landsat-based estimation of mangrove forest loss and restoration in Guangxi province, China, influenced by human and natural factors. *IEEE Journal of Selected Topics in Applied Earth Observations and Remote Sensing*, 8(1): 311–323, doi: [10.1109/JSTARS.2014.2333527](https://doi.org/10.1109/JSTARS.2014.2333527)
- Li Zhen, Zhang Zhiying, Li Jie, et al. 2008. Pollen distribution in surface sediments of a mangrove system, Yingluo Bay, Guangxi, China. *Review of Palaeobotany and Palynology*, 152(1–2): 21–31
- Li Zhen, Saito Y, Mao Limi, et al. 2012. Mid-Holocene Mangrove succession and its response to sea-level change in the upper Mekong River delta, Cambodia. *Quaternary Research*, 78(2): 386–399, doi: [10.1016/j.yqres.2012.07.001](https://doi.org/10.1016/j.yqres.2012.07.001)
- Lorente F L, Pessenda L C R, Oboh-Ikuenobe F, et al. 2014. Palynofacies and stable C and N isotopes of Holocene sediments from Lake Macuco (Linhares, Espírito Santo, southeastern Brazil): depositional settings and palaeoenvironmental evolution. *Palaeogeography, Palaeoclimatology, Palaeoecology*, 415: 69–82, doi: [10.1016/j.palaeo.2013.12.004](https://doi.org/10.1016/j.palaeo.2013.12.004)
- Meng Xianwei, Xia Peng, Li Zhen, et al. 2017. Mangrove development and its response to Asian monsoon in the Yingluo Bay (SW China) over the last 2000 years. *Estuaries and Coasts*, 40(2): 540–552, doi: [10.1007/s12237-016-0156-3](https://doi.org/10.1007/s12237-016-0156-3)
- Monacchi N M, Meier-Grünhagen U, Finney B P, et al. 2009. Mangrove ecosystem changes during the Holocene at Spanish Lookout Cay, Belize. *Palaeogeography, Palaeoclimatology, Palaeoecology*, 280(1–2): 37–46
- Parkinson R W, Delaune R D, White J R. 1994. Holocene sea-level rise and the fate of mangrove forests within the wider Caribbean region. *Journal of Coastal Research*, 10(4): 1077–1086
- Smoak J M, Breithaupt J L, Smith III T J, et al. 2013. Sediment accretion and organic carbon burial relative to sea-level rise and storm events in two mangrove forests in Everglades National Park. *Catena*, 104: 58–66, doi: [10.1016/j.catena.2012.10.009](https://doi.org/10.1016/j.catena.2012.10.009)
- Versteegh G J M, Schefuß E, Dupon L, et al. 2004. *Taraxerol* and *Rhizophora* pollen as proxies for tracking past mangrove ecosystems. *Geochimica et Cosmochimica Acta*, 68(3): 411–422, doi: [10.1016/S0016-7037\(03\)00456-3](https://doi.org/10.1016/S0016-7037(03)00456-3)
- Wooller M J, Morgan R, Fowell S, et al. 2007. A multiproxy peat record of Holocene mangrove palaeoecology from Twin Cays, Belize. *The Holocene*, 17(8): 1129–1139, doi: [10.1177/0959683607082553](https://doi.org/10.1177/0959683607082553)
- Xia Peng, Meng Xianwei, Li Zhen, et al. 2015. Mangrove development and its response to environmental change in Yingluo Bay (SW China) during the last 150 years: stable carbon isotopes and mangrove pollen. *Organic Geochemistry*, 85: 32–41, doi: [10.1016/j.orggeochem.2015.04.003](https://doi.org/10.1016/j.orggeochem.2015.04.003)
- Yulianto E, Sukapti W S, Rahardjo A T, et al. 2004. Mangrove shoreline responses to Holocene environmental change, Makassar Strait, Indonesia. *Review of Palaeobotany and Palynology*, 131(3–4): 251–268